

# Towards local oscillators based on arrays of niobium Josephson junctions

M A Galin<sup>1,2</sup>, A M Klushin<sup>1,2</sup>, V V Kurin<sup>1,2</sup>, S V Seliverstov<sup>3</sup>, M I Finkel<sup>3</sup>,  
G N Goltsman<sup>3,4</sup>, F Müller<sup>5</sup>, T Scheller<sup>5</sup> and A D Semenov<sup>6</sup>

<sup>1</sup>Institute for Physics of Microstructures RAS, 603950 Nizhny Novgorod, Russia

<sup>2</sup>Lobachevsky State University of Nizhny Novgorod, 603950 Nizhny Novgorod, Russia

<sup>3</sup>Department of Physics, Moscow State Pedagogical University, 119992, Moscow, Russia

<sup>4</sup>National Research University Higher School of Economics, 101000 Moscow, Russia

<sup>5</sup>Physikalisch-Technische Bundesanstalt, D-38116 Braunschweig, Germany

<sup>6</sup>Institute of Optical Sensor Systems, German Aerospace Centre (DLR), D-12489 Berlin, Germany

E-mail: [a\\_klushin@ipmras.ru](mailto:a_klushin@ipmras.ru)

Received 10 November 2014, revised 17 January 2015

Accepted for publication 13 February 2015

Published 19 March 2015



CrossMark

## Abstract

Various applications in the field of terahertz technology are in urgent need of compact, wide-tunable solid-state continuous wave radiation sources with a moderate power. However, satisfactory solutions for the THz frequency range are scarce yet. Here we report on coherent radiation from a large planar array of Josephson junctions (JJs) in the frequency range between 0.1 and 0.3 THz. The external resonator providing the synchronization of JJ array is identified as a straight fragment of a single-strip-line containing the junctions themselves. We demonstrate a prototype of the quasioptical heterodyne receiver with the JJ array as a local oscillator and a hot-electron bolometer mixer.

Keywords: Josephson junctions, heterodyne receiver, local oscillator, hot-electron bolometer

(Some figures may appear in colour only in the online journal)

## 1. Introduction

Advances in generation and registration of terahertz waves are essential not only for different fields of sciences such as astronomy and spectroscopy but also for the number of applications such as radiolocation and radio vision, or detecting different objects behind opaque screens or in the fog. Very often measurements in this frequency range are made with heterodyne receivers. A wide variety of mixers available for this regime, e.g. Schottky diodes, tunnel superconductor–isolator–superconductor (SIS) junctions, or hot electron bolometers (HEB), contrasts with only a few types of local oscillators (LO). Solid-state multipliers cover the sub-terahertz portion of the spectrum but suffer lack of power at higher frequencies where gas lasers at fixed frequencies and moderately tunable quantum cascade lasers deliver sufficient power for applications. Most terahertz lasers, however, require external amplitude and phase stabilization. Recently electromagnetic oscillations of Josephson junctions (JJs) have become an alternative technology for the development of LO

in the range from microwaves to terahertz waves. Being first reported almost 50 years ago for a single tunnel junction [1], generation of electromagnetic waves by JJ is now applied in flux-flow oscillators, based on SIS junctions [2]. They provide a power of the order of  $1 \mu\text{W}$  in the frequency range up to 0.7 THz and are therefore best used in on-chip integrated receivers. Even larger power can be achieved by synchronizing oscillations of individual junctions in an ensemble. For example, layered superconductors such as the copper-oxide high-temperature superconductor  $\text{Bi}_2\text{Sr}_2\text{CaCu}_2\text{O}_{8+\delta}$  are emerging as compact sources of coherent continuous-wave electromagnetic radiation in the subterahertz and terahertz frequency ranges [3]. Another promising approach is a planar JJ array. For the array of Nb junctions the off-chip power of almost  $10 \mu\text{W}$  was demonstrated at 0.14 THz [4]. The electrostatics of the planar array has the advantage of supporting effective coupling with the quasioptical Gaussian mode of electromagnetic field. On-chip integration of a heterodyne receiver typically causes an increase in the receiver noise temperature; hence an alternative solution preserving an

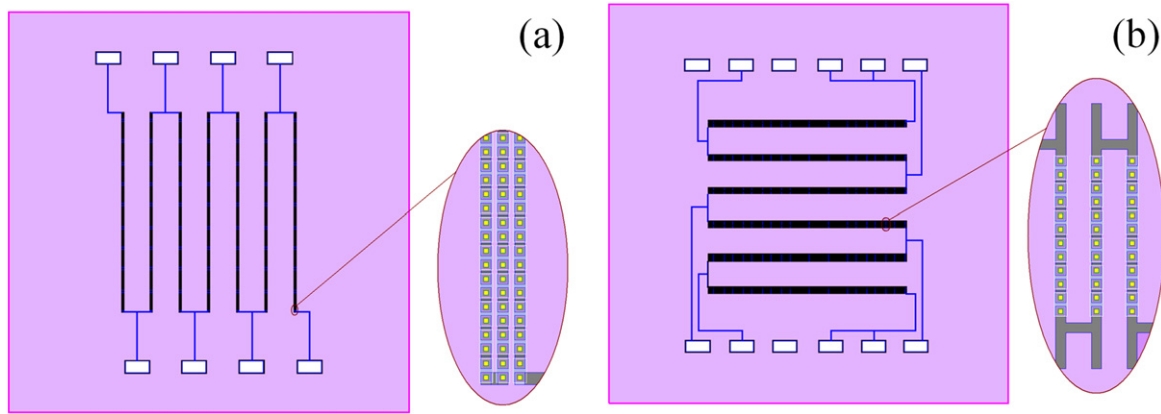


**Figure 1.** Layouts of the 6972 JJ array (a) and the 9000 JJ array (b). Rectangles present dc contact pads. Insets show layout of sub-arrays.

ultimate sensitivity may be a partial integration. In this case coupling out in a quasioptical mode is mandatory because it allows a precise, lossless handling of the generated power and a further coupling to the mixer. The obvious attractiveness of LO from a planar array, as compared to vacuum electronics, solid state sources or quantum cascade lasers, is the straightforward capability for the short-range integration with HEB or SIS mixers. A special advantage of a JJ array LO is the possible tunability in the frequency range which may be in principle much larger than the range covered by state of art solid state sources. The frequency range of a Josephson source is fundamentally limited to the frequency corresponding to the energy gap. This implies the use of high-temperature superconducting materials for sources in the terahertz frequency range. Although the receiver optics, specifically in the case of quasioptical coupling, should be developed for the particular frequency range, there are common elements which can be probed and optimized at lower frequencies. Hence, the readily available Josephson sources made from low-temperature superconducting materials can be used as scalable models for the study and development of future LO in the terahertz frequency range.

In this paper, we report on the JJ array source and its application as LO in the laboratory prototype of a heterodyne receiver at frequencies above 0.1 THz.

## 2. Layout of the JJ arrays

In our experiments series arrays of Nb–Nb<sub>x</sub>Si<sub>1-x</sub>–Nb junctions have been used [5]. Several JJ array chips with different designs were fabricated on 3 inch silicon wafers with a microwave permittivity  $\epsilon_{Si} = 11.9$  and a specific resistance of about  $10 \Omega \text{ cm}$ . All chips have the same dimension of  $10 \times 10 \text{ mm}$  and a thickness of 0.38 mm. A ground plane is often used for synchronizing junctions [6], but our samples don't need it because the silicon substrates are expected to be external resonators themselves. Below we will show that true resonators for series of JJ arrays are straight fragments of a stripline which are formed by the junctions. The dimension of each junction in the array is  $8 \times 8 \mu\text{m}$ , and the distance

between them is  $7 \mu\text{m}$ . The layouts of two samples investigated here are presented schematically in figure 1. The first series array is similar to those described previously [4]. It consists of seven subarrays. Each subarray includes three straight lines spaced by  $18 \mu\text{m}$  and having nearly 5 mm length. The lines are connected in series and contain 332 JJs each (figure 1(a)) so that the total number of junctions is  $N = 332 \times 3 \times 7 = 6972$ . Each subarray can be biased and measured independently. The second circuit design consists of six subarrays. Each of them represents a meandering line which contains 1500 junctions situated in the transverse sections of the meander (figure 1(b)). The length of each of 125 transverse sections of the meanders is nearly  $200 \mu\text{m}$  with 12 junctions. The total number of junctions is  $N = 12 \times 125 \times 6 = 9000$ .

Before being applied as LO the arrays were characterized in a standard helium dewar at 4.2 K. Thin-film contact pads shown in figure 1 allowed us to independently bias and measure generated electromagnetic power from each individual subarray or several selected subarrays. For the express estimate of generated power a detector from crystalline, high-purity *n*-type InSb was used [7]. It was positioned at a distance of 5 mm from the surface of the array. To acquire current-voltage characteristics (*IV* curves) of the arrays, the dc or pulse bias current was used. In the latter case the pulse duration and pulse repetition period were in the ranges from 0.05 to 12 ms and from 80 to 100 ms, respectively, which were produced by the current source Keithley 6221 synchronized with nanovoltmeter Keithley 2182A. The pulse bias current regime allowed us to decrease the sample heating especially for larger arrays [8].

The *IV* curve of 6972 JJ array is shown in figure 2(a). The scale for the Josephson radiation frequency  $f$  was derived from the equation  $f = \Phi_0 V / N$ , where  $\Phi_0$  is the flux quantum and  $V$  is the total voltage drop over the array. The axis with the Josephson frequency is shown next to the voltage axis. The critical current of a single junction  $I_c$  was about 2.1 mA, the corresponding critical current density  $J_c = 3.3 \times 10^3 \text{ A cm}^{-2}$ , and the normal resistance  $R_n \approx 0.1 \Omega$ . Therefore, for a single junction the average characteristic voltage  $V_c = 0.23 \text{ mV}$  and the characteristic frequency

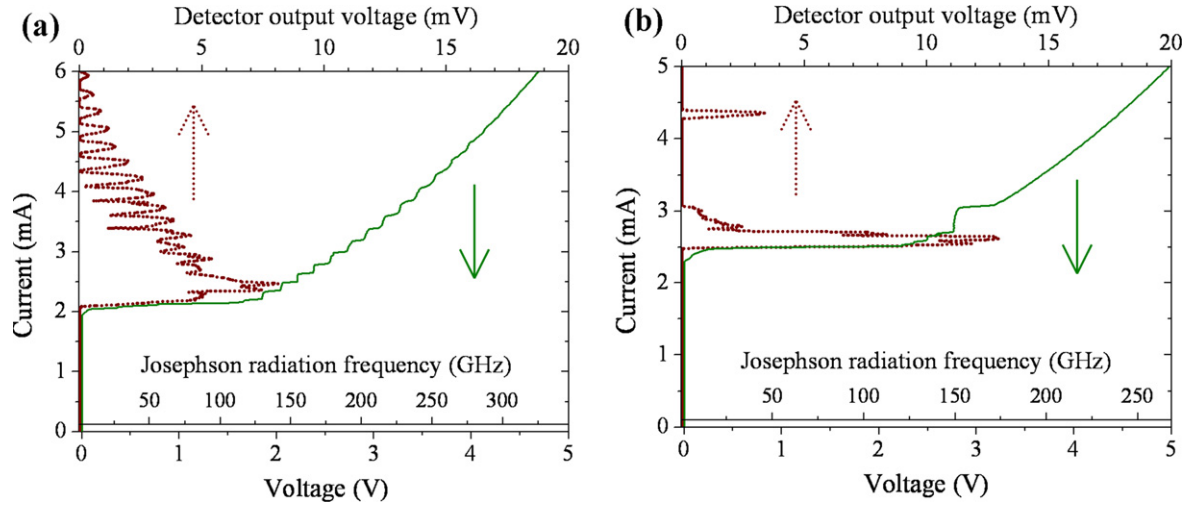


**Figure 2.** *IV* curve and signal voltage of the InSb detector: (a) for the 6972 JJ array and (b) for the 9000 JJ array.

**Table 1.** The characteristics of the first 10 current steps in *IV* curve of 6792 JJ array (see figure 1(a)).

$f_s$ (GHz)	$I_s$ (mA)	$2L/\lambda_{\text{eff}}$
128.8	0.12	10.91
142.1	0.13	12.03
153.5	0.13	13.00
165.1	0.13	13.98
177.4	0.16	15.02
190.8	0.17	16.15
202.5	0.18	17.15
214.4	0.18	18.15
226.4	0.16	19.17
238.8	0.18	20.22

$f_c = 111$  GHz. The output voltage of the n-InSb detector  $V_{\text{det}}$  which is proportional to the detected electromagnetic power  $P_{\text{det}}$  is depicted in the same figure. It is seen that the *IV* curve contains series of current steps and the maxima of the Josephson radiation received by InSb detector correspond to the step voltages. It is easy to see that the voltage difference between the adjacent steps  $\Delta V$  is nearly constant. Such steps can be interpreted as cavity steps [9, 10] which correspond to the resonance of Josephson oscillations with eigenmodes of some resonator. In our case the voltage step spacing corresponds to mode frequency spacing of the multimode single-strip-line (SSL) resonator which is formed by 332 JJ straight arrays so that current steps are actually self-induced. The SSL resonator length  $L$  is related with the fundamental resonance mode frequency as  $f_0 = c/(2L\sqrt{\epsilon_{\text{eff}}})$ , where  $c$  is the light speed,  $\epsilon_{\text{eff}} = \sqrt{(\epsilon_{\text{Si}} + 1)}/2$  is the effective dielectric permittivity, so for  $L = 5$  mm we have  $f_0 = 11.8$  GHz. This value is very close to the observed frequency difference between the adjacent steps with the average accuracy of 5%. In table 1 we listed frequencies  $f_s$  and current amplitudes  $I_s$  for the first ten steps. The last column demonstrates that the ratio of the length  $L$  of SSL resonator to the effective half-wavelength defined as  $\lambda_{\text{eff}}/2 = c/(2f\sqrt{\epsilon_{\text{eff}}})$  is nearly integer for each step.

It is remarkable that in spite of existing self-induced cavity steps, which are usually considered as an indication of standing waves, the presence of a relatively weak travelling component of the electromagnetic field can be sufficient to synchronize all junctions including those, which are situated in the vicinities of minima of standing waves.

It should be noticed that we did not observe on *IV* curves any fine details making evident coupling to dielectric cavity formed by dielectric silicon substrate as it has been reported by us earlier [4]. Nevertheless, the substrate can act as an additional resonator but its role in the synchronization effectiveness of the series JJ array will have to be revealed in future.

As the frequency increases, self-induced steps become less legible and the detector signal  $V_{\text{det}}$  decreases rather rapidly (figure 2(a)). Taking into account the conversion factor of  $200 \text{ V W}^{-1}$  for our InSb detector [11], we obtained that  $P_{\text{det}}$  decreases from at least  $40 \mu\text{W}$  at 143 GHz to approximately  $2 \mu\text{W}$  at 320 GHz. We associate this remarkable decrease of  $P_{\text{det}}$  with the microwave absorption in our silicon wafers having small specific resistance 1–10  $\Omega \text{ cm}$ .

The *IV* curve of 9000 JJ array is depicted in figure 2(b). It looks completely different from the previous case of the 6972 JJ array though the parameters of individual junctions  $I_c$ ,  $J_c$ ,  $R_n$ ,  $V_c$  and  $f_c$  are close for both samples. The main difference is that there are no steps which can be associated with the whole length of SSL resonator but there are groups of steps in the range from 120 to 150 GHz, a big step at 150 GHz and a small step at 240 GHz. All of them can be attributed to half-wavelength and one-wavelength resonances of the transversal  $200 \mu\text{m}$  part of the meander line containing 12 JJs together with two terminating  $40 \mu\text{m}$  strips (see figure 1(b), inset).

The step at 150 GHz has large current magnitude  $I_s = 0.33$  mA, the step at 240 GHz is considerably smaller so it is hardly readable in figure 2(b). The largest detected power  $P_{\text{det}} = 65 \mu\text{W}$  was obtained in the vicinity of the small step at the frequency  $f = 134$  GHz (figure 2(b)). At the large self-induced step at the frequency  $f = 150$  GHz, the detected power decreased to  $P_{\text{det}} = 12 \mu\text{W}$ . At the frequency 240 GHz a power

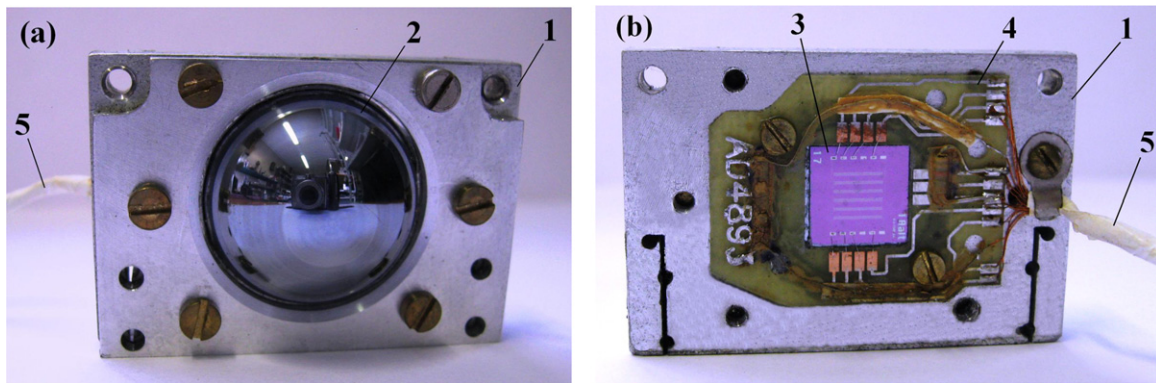


**Figure 3.** Front (a) and rear (b) sides of the JJ array holder: (1) aluminium case; (2) silicon lens; (3) chip with the array; (4) printed circuit board; (5) connecting dc cable.

up to  $17 \mu\text{W}$  was detected. Such peculiarities of  $IV$  curve and radiated power of meander Josephson transmission line can be understood in terms of periodically inhomogeneous Josephson transmission lines just as it was done in [12]. As the spectrum of periodically inhomogeneous line has the band character and eigenmodes are the Bloch waves [13], the steps position on the  $IV$  curve and the corresponding radiation efficiency can be associated with the resonances at the edges of the Brillouin zone which just correspond to the meander cuts. At such frequencies the mode group velocity has the minimal value that promotes energy accumulation. Also due to low group velocity the damping rate on the unit length gets higher and we have a regime of nearly travelling wave in the line and it is the reason why we did not observe the resonances associated with the total length as we did with the first array design. Due to such probable travelling wave regime all junctions in the line feel the identical electromagnetic environment that promotes their full synchronization. Such a regime of travelling wave opens a possibility of synchronization of practically unlimited number of junctions. In both cases the mixture of travelling and standing waves is sufficient to provide full synchronization of JJ array despite the seeming nonequivalence of junction positions.

Further we use the second array containing 9000 junctions as LO because of its better efficiency.

### 3. Receiver setup scheme and noise temperature measurement

To make use of JJ array as a practical LO, its generated electromagnetic radiation has to be collected and overlapped with the radiation from the signal channel of a heterodyne receiver. To achieve this we glued the substrate with the 9000 JJ array on the flat rear side of an elliptical silicon lens (figure 3). We tested two silicon lenses with the same geometric parameters but different specific resistances of  $40 \Omega \text{ cm}$  (low-resistance lens) and  $40 \text{ k}\Omega \text{ cm}$  (high-resistance lens). Both lenses were made from non-compensated silicon. The accuracy of positioning the geometrical center of the array into the geometric focus of the lens ellipse was  $\pm 10 \mu\text{m}$ . The lens was pressed down against an aluminium case, which

was installed in the vacuum chamber of an optical helium-bath cryostat. A printed circuit board with an opening for the chip was located on the case surface and provided mechanical support for the dc connections (figure 3(b)). To prevent capturing magnetic flux by the JJ array, the case was surrounded with a  $\mu$ -metal shield. To reduce heating of the sample, IR radiation was blocked by two Zitex G106 infrared filters [14] at 77 and 4.2 K. Inside the cryostat the case was located at a distance of 60 mm from Mylar vacuum-tight window with a diameter of 45 mm. As a result we were able to operate our array at a constant temperature that depended on the bias current but remained in the range 4.4–5 K.

Using two silicon lenses with different specific resistance we probed the radiation power from the 9000 JJ array by the Agilent sensor W8486A. To couple the power to the sensor we use the Teflon lens with the diameter of 80 mm and focal distance of 53 mm. Moving the Teflon lens along the line connecting the flared end of the waveguide of the sensor and the window of the cryostat we got the maximum detected power. With the low-resistance silicon lens no Josephson radiation was detected outside of the cryostat. Contrary, using the high-resistance lens we detected up to  $4.5 \mu\text{W}$  radiation power. Such a striking difference between two lenses with various specific resistances supports our suggestion that the microwave absorption in the low-resistance silicon substrate may be the main reason of the weak Josephson radiation from our JJ array samples at higher frequencies.

We used quasioptical HEB [15] as the mixer. It was made from a NbN/Au bilayer deposited in a single technological vacuum cycle (*in situ*) onto a silicon substrate. The thicknesses of NbN and Au films were 3.5 and 15 nm, respectively. The gold layer was then partly removed by ion and chemical etching through a window in the electron resist which defines the sensitive area of the microbolometer. The dimensions of the microbolometer along (length) and perpendicularly (width) to the current flow between the antenna terminals were 0.2 and  $1.5 \mu\text{m}$ , respectively. The sheet resistance of NbN film was about  $500 \Omega/\text{sq}$ . The applied length-to-width ratio of the sensitive area provided a good RF coupling between the bolometer and the log-spiral antenna. The radiation was coupled to the antenna with a silicon lens. A mixer block with HEB was mounted onto the cold plate of

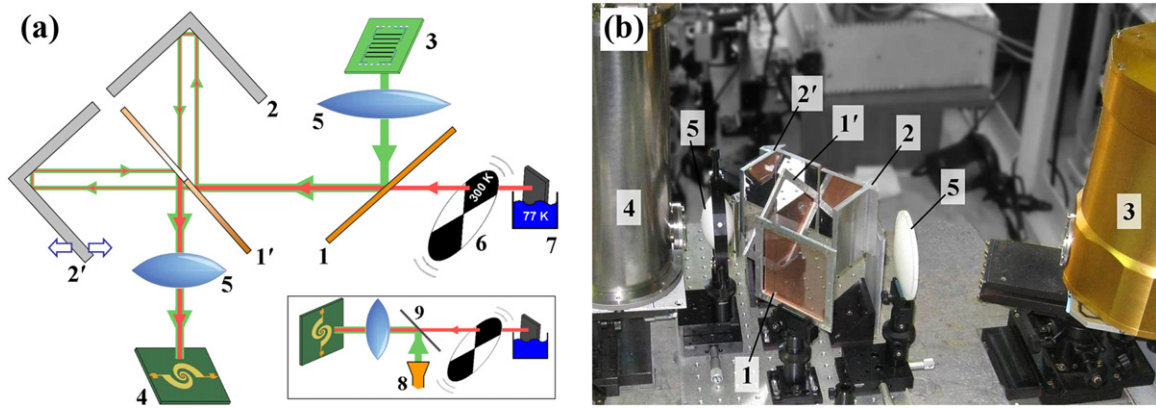


**Figure 4.** (a) Diagram of the laboratory heterodyne receiver with the Martin–Puplett interferometer: (1) vertical oriented and (1′) 45° oriented grid polarizers; (2) fixed and (2′) movable roof mirrors; (3) JJ array LO (inside the cryostat); (4) HEB mixer (inside the cryostat); (5) Teflon lenses; (6) chopper wheel; (7) 77 K load. The inset shows the reference setup: (8) multiplier LO; (9) beam-splitter. Part of the diagram is imaged on photo (b).

another optical liquid helium cryostat with a 0.5 mm thick high-density polyethylene window and four cold Zitex G104 filters cutting off the background radiation. Intermediate frequency chain contained a broadband bias tee, a low noise amplifier with a noise temperature of about 5 K and a gain of 30 dB across the intermediate frequency band of 1.35–1.75 GHz.

A photo and a schematic diagram of the receiver prototype are presented in figure 4. We used a Martin–Puplett interferometer (MPI) [16, 17] as a diplexer in order to combine an input signal from the alternating thermal load and the LO radiation. Using the MPI provides transformation of the electromagnetic power of linear polarized JJ radiation to circular polarized output signal for lossless coupling with the log-spiral antenna. Another advantage of MPI is that it delivers total power of both the LO and the signal source to the mixer. It enables us to avoid the loss of relatively weak LO radiation that has to occur on classical beam splitters. Additional Teflon lenses on both LO and mixer sides matched the beam in the interferometer to the directional pattern of the integrated lens-antennas. To align the diplexer for LO radiation and measure its directional pattern we used zero-bias Schottky diode detector [18]. The radiation pattern of the JJ array LO has a complex asymmetric structure that includes several lobes emerging from the silicon lens at different angles to the optical axis. Depending on the frequency, the angle as well as the portion of the total LO power associated with the certain lobe vary, hence making it difficult to keep the optical coupling to the diplexer constant. The external Teflon lenses provide a total frequency independent waist with an almost Gaussian power distribution at the position of the mixer. They were set at focal distances from the JJ array and detector samples that were 306 and 53 mm respectively. To attain a maximum pumping of HEB the cryostat with JJ array was turned to the angle near 30° as seen in figure 4(b). As a reference LO we used a semiconductor multiplier in combination with a Mylar beam splitter that required minor

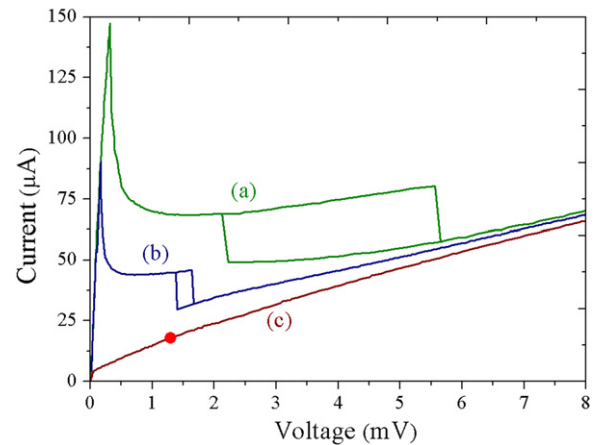


**Figure 5.** Current-voltage characteristics of the mixer: unpumped (a), pumped with some LO power (b), optimally pumped with JJ array LO (c). The bold point marks the operation point, where the smallest noise temperature was achieved.

changes in the setup. They are depicted in the inset of figure 4(a). The LO frequency in this case was 140 GHz.

The Y-factor technique was used to determine the receiver noise temperature with both the JJ array and the multiplier. The Eccosorb plate decorated with 7 mm high pyramidal elements served as a thermal load.

Figure 5 depicts the evolution of the unpumped *IV* curve of HEB to the optimally pumped curve with the increase in the power of the JJ array LO at 134 GHz. Substituting the JJ array LO and MPI with the semiconductor LO and the beam splitter, we obtained a pretty similar optimally pumped *IV* curve. In both cases, the measurement of non-corrected Y-factor at the optimal bias of 1.3 mV (bold point in figure 5) gave the value of 1.09 corresponding to the noise temperature of 2400 K. There are a few reasons for getting this relatively large noise temperature in our setup. First the material of our thermal load is not a perfect black body radiator at frequencies around 0.1 THz [19]. The second reason is the operation of HEB mixer at frequencies less than the value of

660 GHz corresponding to the superconducting energy gap of the NbN film at 4.2 K [20]. The HEB responds differently to the subgap radiation and to the radiation with the quantum energy well above the superconducting energy gap [21]. The difference is also clearly seen between optimally pumped *IV* curves when they are obtained with the millimeter wave LO (figure 5) and the terahertz LO [22]. Besides that the planar log-spiral antenna of our HEB mixer was optimized for higher frequencies. At 2.5 THz the double sideband noise temperature of 600 K has been reported for the same NbN HEB [23]. At lower frequencies the impedance mismatch between the antenna and the mixer increases resulting in larger coupling losses. We rule out the lack of the phase synchronization of the JJ array since the same noise temperature was measured with the solid state LO. Finally, successful pumping of the HEB mixer by the off-chip JJ array LO at 0.1 THz confirms the possibility of developing partly integrated quasioptical heterodyne receivers combining HEB and JJ array at THz frequencies.

#### 4. Conclusion and outlook

We investigated the Josephson radiation from two planar arrays of niobium JJs with different layouts. In both cases, current steps in the *IV* curves were caused by self-synchronization of junctions in the repetitive subarrays of the whole structure which acted as external SSL resonator. We suggested that in both samples considered field distribution contains a considerable travelling component that excludes deep field minima and provides full synchronization of all junctions independently of their position in the lines. We demonstrated successful pumping of the HEB mixer by Josephson radiation of such an array at frequencies above 0.1 THz. The integration of the JJ array LO and the HEB mixer on the same cryogenic platform is our further goal. The major challenge of integration is the possibility to use a smaller MPI. Propagating weakly divergent Gaussian beams over a long distance outside the cryostat requires to have large diameter of the beam and, correspondingly, large optical path inside the MPI. This optical path restricts the available bandwidth at the intermediate frequency of a heterodyne receiver. Integrating in one cryogenic platform also drastically reduces the cost of commercial developments. The total input dc power required by the array is less than 15 mW that favours a closed-cycle mechanical cryocooler.

#### Acknowledgments

The work was supported by The Ministry of Education and science of Russian Federation, project № 8837 and project № 14.740.11.0889, and by the grant (the agreement of August

27, 2013 no. 02.B.49.21.0003 between The Ministry of education and science of the Russian Federation and Lobachevsky State University of Nizhni Novgorod). Also it was partly supported by the grant of Russian Foundation for Basic Research N15-02-05793, by the Ministry of Education and Science of Russian Federation under contracts no. 14. B25.31.0007, no. 3.2575.2014/K, and state task no. 960, by the Russian Federation President Grant for Leading Scientific Schools #1918.20.2014.2 and by the Swedish Foundation for International Cooperation in Research and Higher Education. The authors thank Maxim Yu Levichev, Vadim A Markelov and Anna I El'kina for their contributions to the development and construction of the quasioptical heterodyne receiver setup.

#### References

- [1] Yanson I K, Svistunov V M and Dmitrenko I M 1965 *Zh. Eksp. Teor. Fiz.* **48** 976  
Yanson I K, Svistunov V M and Dmitrenko I M 1965 *Sov. Phys.-JETP* **21** 650
- [2] Koshelets V P and Shitov S V 2000 Integrated superconducting receivers *Supercond. Sci. Technol.* **13** R53–69
- [3] Welp U, Kadowaki K and Kleiner R 2013 *Nat. Photonics* **7** 702
- [4] Song F, Müller F, Scheller T, Semenov A D, He M, Fang L, Hübers H-W and Klushin A M 2011 Compact tunable sub-terahertz oscillators based on Josephson junctions *Appl. Phys. Lett.* **98** 142506
- [5] Mueller F, Behr R, Weimann T, Palafox L, Olaya D, Dresselhaus P D and Benz S P 2009 *IEEE Trans. Appl. Supercond.* **19** 981
- [6] Barbara P, Cawthorne A B, Shitov S V and Lobb C J 1999 Stimulated emission and amplification in Josephson junction arrays *Phys. Rev. Lett.* **82** 1963
- [7] Kinch M A and Rollin B V 1963 *Br. J. Appl. Phys.* **14** 672
- [8] Song F, Müller F, Behr R, Fang L and Klushin A M 2011 Self-emission from arrays of overdamped Josephson junctions *IEEE Trans. Appl. Supercond.* **21** 315–18
- [9] Dayem A H and Grimes C C 1996 *Appl. Phys. Lett.* **9** 47
- [10] Longacre J A 1979 *J. Appl. Phys.* **50** 6451
- [11] Vystavkin A N, Gubankov V N, Listvin V N and Migulin V V 1968 *Radiophys. Quantum Electron.* **11** 334  
Vystavkin A N, Gubankov V N, Listvin V N and Migulin V V 1968 *Izv. Vuz. Radiofiz.* **11** 602
- [12] Baryshev A M, Julin A V, Kurin V V, Koshelets V P, Dmitriev P N and Filippenko L V 1999 Forward and backward waves in Cherenkov flux-flow oscillators *Supercond. Sci. Technol.* **12** 967–69
- [13] Ramo S, Whinnery J R and Van Duzer T 1967 *Fields and Waves in Communication Electronics* (New York: Wiley)
- [14] Benford D J, Gaidis M C and Kooi J W 2003 *Appl. Opt.* **42** 5118
- [15] Shurakov A, Seliverstov S, Kaurova N, Finkel M, Voronov B and Goltsman G 2012 Input bandwidth of hot electron bolometer with spiral antenna *IEEE Trans. Terahertz Sci. Technol.* **2** 400–5
- [16] Martin D and Puplett E 1970 *Infrared Phys.* **10** 105
- [17] Lesurf J.C.G. 1981 *Infrared Phys.* **21** 383

- [18] Semenov A, Cojocari O, Hübers H-W, Song F, Klushin A and Muller A S 2010 Application of zero-bias quasi-optical schottky-diode detectors for monitoring short-pulse and weak terahertz radiation *IEEE Electron Device Lett.* **31** 674–6
- [19] Halpern M, Gush H P, Wishnow E and de Cosmo V 1986 *Appl. Opt.* **25** 565
- [20] Lobanov Y, Tong E, Blundell R, Hedden A, Voronov B and Gol'tsman G 2011 Large-signal frequency response of an HEB mixer: from 300 MHz to terahertz *IEEE Trans. Appl. Supercond.* **21** 628–31
- [21] Semenov A D, Hübers H-W, Schubert J, Gol'tsman G N, Elantiev A I, Voronov B M and Gershenzon E M 2000 Design and performance of the lattice-cooled hot-electron terahertz mixer *J. Appl. Phys.* **88** 6758–67
- [22] Hajenius M, Baselmans J J A, Baryshev A, Gao J R, Klapwijk T M, Kooi J W, Jellema W and Yang Z Q 2006 *J. Appl. Phys.* **100** 074507
- [23] Tretyakov I, Ryabchun S, Finkel M, Maslennikova A, Kaurova N, Lobastova A, Voronov B and Gol'tsman G 2011 Low noise and wide bandwidth of NbN hot-electron bolometer mixers *Appl. Phys. Lett.* **98** 033507